System-Level Analysis of IEEE 802.11ah Technology for Unsaturated MTC Traffic

Aleksandr Ometov[†], Nader Daneshfar[†], Ali Hazmi[†], Sergey Andreev[†], Luis Felipe Del Carpio[‡], Parth Amin[‡], Johan Torsner[‡], Yevgeni Koucheryavy[†], and Mikko Valkama[†]

Contact e-mail: aleksandr.ometov@tut.fi

[†] A. Ometov, N. Daneshfar, A. Hazmi, S. Andreev, Y. Koucheryavy and M. Valkama are with the Dept. of Electronics and Communications Engineering, Tampere University of Technology, Korkeakoulunkatu 10, Tampere, FI-33720, Finland
E-mails: aleksandr.ometov@tut.fi, nader.daneshfar@tut.fi, ali.hazmi@tut.fi, sergey.andreev@tut.fi, yk@cs.tut.fi, mikko.e.valkama@tut.fi

[‡] L. F. Del Carpio, P. Amin and J. Torsner are with Ericsson Research, Jorvas, FI-02420, Finland
E-mails: felipe.del.carpio@ericsson.com, parth.amin@ericsson.com, johan.torsner@ericsson.com

Abstract:
Enabling the Internet of Things, machine-type communications (MTC) is a next big thing in wireless innovation. In this work, we concentrate on the attractive benefits offered by the emerging IEEE 802.11ah technology to support a large number of MTC devices with extended communication ranges. We begin with a comprehensive overview of the novel features introduced by the latest IEEE 802.11ah specifications followed by development of a powerful mathematical framework capturing the essential properties of a massive MTC deployment with unsaturated traffic patterns. Further, we compare our analytical findings for a characteristic MTC scenario against respective system-level simulations across a number of important performance indicators. Our analytical results provide adequate performance predictions even when simulations are challenged by the excessive computational complexity. In addition, we study the novel IEEE 802.11ah mechanisms offering improved support for massive device populations and conclude on their expected performance.

Keywords: IEEE 802.11ah; analytical modelling; simulations; MTC/M2M; unsaturated traffic; throughput; delay; power consumption.

1 Introduction and Background

Machine-type (a.k.a. machine-to-machine) communications (MTC) is an enabling technology for the Internet of Things, which features fully automatic data generation, exchange, processing, and actuation among intelligent machines, without or with low intervention of humans [1, 2]. Fuelled by the rapid proliferation in types and numbers of embedded devices, MTC has the potential to revolutionise autonomous wireless connectivity across the verticals of industrial and agricultural automation, transportation, surveillance, healthcare, animal monitoring, smart metering, and many others [3, 4]. Consequently, MTC, already seeing the annual growth of 20%, is expected to develop into an unprecedentedly large market with over trillion-dollar revenues by the year 2020 [5].

In light of the above, it becomes increasingly important to ensure that MTC provides efficient support for various market scenarios by delivering affordable wireless connectivity at low power and with moderate large-scale deployment effort. However, connecting massive numbers of unattended machines with diverse functionalities has proven to be challenging primarily due to the unique characteristics and requirements of MTC. Indeed, while conventional

wireless communication systems have historically been optimised for human-centric communications, with the corresponding emphasis on voice/video and data sessions, MTC transmissions typically carry infrequent and small data, often in delay-tolerant manner.

Therefore, wireless industry had to take decisive steps in order to adapt existing radio access technologies for MTC by improving both their efficiency and reliability. In particular, long-range mobile cellular systems (e.g., HSPA and LTE) have seen numerous enhancements as the result of recent 3GPP standardization activity and related research efforts. The associated modifications range from overload protection schemes and lightweight signalling procedures, to efficient small data transmission and coverage extension mechanisms, as well as advanced approaches to MTC-aware radio resource allocation. Alternatively, multiple short-range radio technologies for wireless sensor networking have evolved to all compete for the MTC niche, but still remain without a distinct leader. These include ZigBee, 6LoWPAN, IEEE 802.15.4, WiFi, Bluetooth low energy, and a plethora of proprietary wireless solutions.

Given that connectivity in licensed cellular bands is expensive and that current short-range unlicensed-band solutions fail to efficiently support a wide variety of MTC use cases with their diverse operational requirements, the wireless community has been seeking for a novel effective MTC-focused radio access technology. To this end, it has soon been recognised that the favourable propagation properties of low-frequency spectrum at sub 1 GHz may provide improved communication ranges when compared to, e.g., conventional WiFi protocols operating at 2.4 and 5 GHz bands [6, 7], as it is presented in Fig. 1. However, the available spectrum at sub 1 GHz license-exempt ISM bands is extremely scarce and hence requires careful system design considerations [8].

With this in mind, after outlining the purpose and the technical scope of the novel IEEE 802.11ah project, the standardization work of the corresponding TGah task group has commenced in November 2010. The planned technology, which is generally based on down-clocked version of IEEE 802.11ac standard, is currently being finalised to enable low-cost and long-range connectivity across massive MTC deployments with high spectral and energy efficiencies. Today, thousands of MTC devices may already be found in dense urban areas, smart grids [9], and airports [10], which has demanded respective protocol modifications.

Fortunately, IEEE 802.11ah technology does not need to maintain the backwards compatibility with the other representatives of IEEE 802.11 family (both conventional 802.11a/b/g/n and more recent 802.11ac solutions). As 802.11ah operates over different frequencies than the existing 802.11 systems, TGah could afford defining novel compact frame formats, as well as offering more efficient mechanisms to support a large number of devices, advanced channel access schemes, together with important power saving and throughput enhancements. As a result, 802.11ah is believed to significantly enrich the family of 802.11 protocols, which already receive increasing attention from mobile network operators willing to introduce low-cost connectivity in unlicensed bands thus augmenting their cellular deployments [10].

The emerging 802.11ah technology has already captured attention of both industry and academia, with a recent avalanche of research literature on the topic, as it is expected to be finalized and meet the market in 2017. The corresponding publications reviewed the physical-layer features of 802.11ah, when applied to both rural [11] and urban [12] use cases, delivered the link budget and quantified the outage probabilities. Additionally, they covered important challenges faced by the TGah standardization activities [13] and proposed related improvements for MIMO-OFDM design [14], as well as showed the operation of system prototypes [10]. The performance of 802.11ah technology has also been compared with that of ZigBee to indicate the crucial areas for improvement [15, 16].

Further, system-level capacity analysis has been conducted in [17], and the follow-up works have introduced a comprehensive overview of 802.11ah technology [18, 19, 20], as well as proposed novel channel access protocols for collision avoidance/resolution [21, 22] and dense MTC deployments [23]. Of particular interest has been the focus on improved contention-based access with grouping of MTC devices [24] and then managing the performance of such groups [25]. Additionally, efficient redundancy-check codes for 802.11ah have been designed [26].

Most importantly, many latest publications have concentrated on improved energy efficiency of relatively short-range 802.11ah technology, from energy harvesting [27] and conservation [28] schemes to enhanced power saving modes [29] and mechanisms [30, 31]. As follows from our survey, existing research efforts have so far been targeting physical-layer and other special-case improvements, as well as full-buffer system capacity evaluations.

However, a comprehensive system-level 802.11ah analysis, mindful of MTC-specific traffic dynamics and realistic contention between a large numbers of devices, is currently missing in the existing literature. Conventional approaches to assess 802.11 family of protocols are mainly focused on saturated analysis due to its mathematical simplicity. For instance, the well-known work by Bianchi and Tinnirello [32] also follows a similar approach based on Markov chains but mainly focuses on the saturated case. There have been other works on the full-buffer analysis [33, 34] but academia is still facing a lack of research results in low arrival rate regime. In fact, these results are rather limited and mainly focus on the throughput analysis [35].

After an extensive literature overview, we discovered only a few works addressing the unsaturated IEEE 802.11ah operation analysis. In [36], the authors elaborate on the modification of channel access mechanisms for non-full buffer scenarios and propose a simple model based on the duty cycle limitation

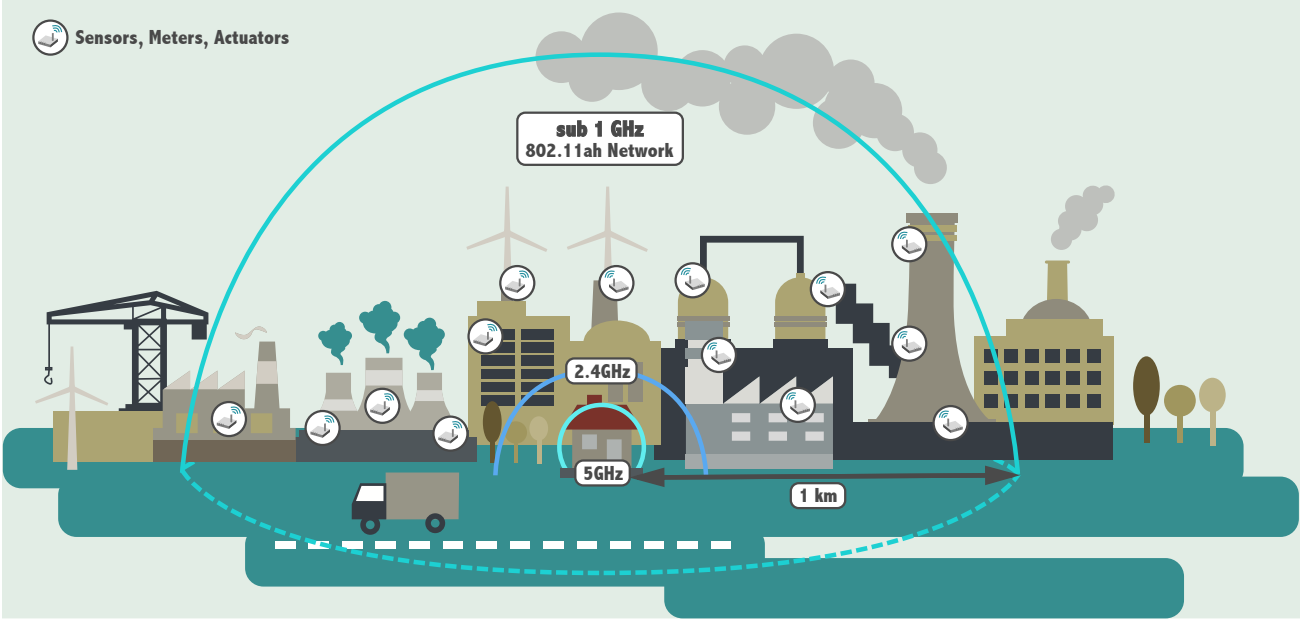

Figure 1 A characterisic large-scale MTC scenario

approach. A complete analytical model for unsaturated scenario is not provided in that work but the problem statement is indicated clearly. Another research that considers unsaturated behavior of the discussed protocol [37] is mainly focused on the hidden node problem and proposes a grouping solution based on the packet generation rate.

In this paper, we bridge the indicated gap by proposing a **novel mathematical framework** for the analysis of a 802.11ah-based system with a high population of nodes by taking into account their unsaturated traffic patterns. The rest of the paper is organised as follows. First, we overview possible 802.11ah applications in the following section. Further, main 802.11ah protocol features are described in Section III. Next, protocol operation is discussed in a characteristic MTC scenario. Then, our system model is introduced and its main analytical assumptions are outlined. These are followed by rigorous analytical derivations, whereas the final section offers a description of the employed simulation environment together with a thorough comparison between analytical and simulation results. Conclusion elaborates on the lessons learned.

2 Prospective IEEE 802.11ah Applications

This section offers an introductory vision on potential IEEE 802.11ah based real-life applications as well as the corresponding benefits of its utilization with respect to the network traffic behavior. The discussed protocol is being developed primarily to satisfy the requirements of a large number of nodes and hence its main use case is related to wireless sensor networks. Other applications are backhaul sensor and metering networks, as well as extended coverage for WiFi family protocols [38]. We further elaborate on both saturated and unsaturated cases.

Saturated scenario could be considered for capacity demanding applications, i.e. video/audio streaming [39], data offloading [40], emergency situations [41], etc. In this case, each station involved into the communication process is assumed to have its buffer full, that is, a packet ready for transmission at any moment of time [42]. As soon as packets are in conflict while being transmitted over the wireless medium, the channel becomes saturated and the transfer delay grows significantly. This work considers the discussed case as not representing the design targets of the protocol directly as it is explained below.

On the other hand, practical IEEE 802.11ah applications are more related to unsaturated scenarios, when a wireless node is transmitting its small packet during a relatively long period of time, which reflects most of today's M2M/MTC operations [6, 30]. In this case, the packet buffer is expected to be empty for most of the observation time and this case is referred to as *unsaturated* scenario. The main corresponding applications of non-full buffer setup are listed below.

- *Smart metering:* IEEE 802.11ah is expected to improve over performance of conventional short-range wireless technologies [43], such as Zigbee, NFC, Bluetooth, etc. The main applications to be supported are: environmental monitoring, smart grids, industrial automation, and healthcare. Keeping in mind the need to serve a large number of communicating devices, the discussed technology proposes novel techniques to reduce the number of collisions and augment the energy efficiency [8].
- *Cellular offloading and extended coverage:* One of the potential benefits of the considered technology is its coverage range of up to 1 km due to the use of sub-GHz frequencies [18]. This feature allows to provide additional possibilities to conventional cellular users by offering

them a certain level of service in extreme cases. In contrast to high-throughput IEEE 802.11ac and 802.11n protocols, lower data rates of 802.11ah may be applicable in cases of national security and public safety [44].

- *Backhaul networks:* Simple IEEE 802.11ah system design allows to link a sub-GHz aggregation point together with its connected nodes to a conventional wireless network [12]. For example, IEEE 802.11g is capable of providing connectivity between the access point and the remote server, while IEEE 802.11ah can offer a wireless backhaul link to accommodate the aggregated traffic generated by the leaf sensors [45].

The above list of applications benefiting from IEEE 802.11ah technology is expected to grow further over time. According to currently available literature, the prospective applications mostly represent the cases of unsaturated traffic behavior.

3 Overview of IEEE 802.11ah Features

This section describes the main MAC and PHY operation as introduced by IEEE 802.11ah specifications based on the latest draft of the standard in [46]. In particular, we introduce novel IEEE 802.11ah protocol features.

3.1 IEEE 802.11ah PHY Features

Importantly, many of the proposed PHY-layer modifications are inspired by past IEEE 802.11 releases. Specifically, the emerging IEEE 802.11ah technology is expected to operate over the sub 1 GHz ISM band. Given that the spectrum availability in this band varies from one country to another, IEEE 802.11ah channelization is currently defined as 863-868 MHz in Europe, 916.5-927.5 MHz in Japan, 755-787 MHz in China, 917.5-923.5 MHz in South Korea, 866-869 MHz and 920-925 MHz in Singapore, as well as 902-928 MHz in the US. For more details, refer to the current version of the standard [46].

Generally, IEEE 802.11ah technology can be regarded as a down-clocked version of the IEEE 802.11ac specification, which is in turn an extension of IEEE 802.11n standard. Basically, IEEE 802.11ah is defined as utilizing the 10-times down-clocking of existing IEEE 802.11ac channel bandwidths, i.e. 2 MHz, 4 MHz, 8 MHz, and 16 MHz channels are currently envisioned. In order to improve the transmission ranges, IEEE 802.11ah additionally introduces a new communication mode employing 1 MHz channel bandwidth.

3.2 IEEE 802.11ah MAC Features

In a nutshell, IEEE 802.11ah has introduced a number of MAC-layer features to comprehensively address the requirements of today's high-density MTC deployments. The key MAC enchantments may be grouped into the four distinct classes discussed further on.

3.2.1 Improved power saving operation

IEEE 802.11ah documentation defines two power saving strategies, referred to as *Non-TIM* and *TIM* operating modes. Accordingly, the MTC devices can be named Non-TIM and TIM station (STAs).

In case of a Non-TIM mode, the IEEE 802.11ah device does not receive the *Traffic Indication Map* (TIM) *information element* (IE) from the beacon frames that are regularly broadcasted by the Access Point (AP). Generally, the TIM IE is used by the AP to indicate whether it has buffered some downlink data for a particular STA. A Non-TIM STA has to send a PS-Poll frame to the AP, thus requesting the delivery of any previously-buffered downlink data. The TIM STAs, however, receive periodic TIM IEs from the beacon frame to detect whether the AP has any buffered data for them. When such a STA detects that the AP has pending data, it sends a PS-poll frame to request the downlink traffic delivery.

IEEE 802.11ah introduces the corresponding improvements to the PS-Poll mechanism to benefit from these power saving schemes. In addition, it extends the time during which the AP does not disassociate a STA if it does not receive any frame from it, namely, the maximum idle period. Furthermore, a Null Data Packet (NDP) paging scheme is developed in order to minimize the time that a given STA can spend in the stand-by mode to check if there is incoming data. It enables any IEEE 802.11ah device, which is expecting the incoming frames, to minimize its wake-up duration by using a paging frame that is significantly shorter compared to a beacon.

The second power saving technique introduced by IEEE 802.11ah is referred to as the Target Wake Time (TWT) that allows a given MTC device to sleep for particular periods of time and then wake up at pre-scheduled instants. It is made to enable the exchange of information with its associated AP at the particular target time. These moments are negotiated in advance between the two communication entities.

3.2.2 Support for a large number of devices

The current version of the specification defines TIM as a bitmap having a feature of uniquely mapping to the STAs *Association Identifier* (AID). We assume that the maximum packet payload of the IE equals to 256 bytes [47, 48], hence a total of approximately two thousand AIDs can be supported. However, as envisioned by IEEE 802.11ah requirements, up to 6000 MTC devices need to be accommodated in some scenarios.

The hierarchical TIM bitmap and TIM segmentation features have been adopted by IEEE 802.11ah specifications to support higher numbers of networked nodes. The hierarchy of TIM comprises 4 pages, each containing 32 blocks. Each block is further divided into 8 sub-blocks of 8 bits each. A STA is identified by its page index, block index within the page, sub-

block index within the block, and its bit position within the sub-block. Further, the address of the STA is encoded in its AID. In order to efficiently encode the TIM, IEEE 802.11ah defines three encoding procedures, namely, Block Bitmap, Single AID, and Offset Length Bitmap Mode.

Further improving the system performance for scenarios where a large number of MTC devices are transmitting their small data packets, IEEE 802.11ah standard adopts overhead reductions in the MAC headers (a.k.a. Header Compression). To this end, a short MAC header format has been defined; the size of the MAC header for a typical 802.11 data frame is 28 bytes, which has been reduced to 18 bytes in IEEE 802.11ah. Finally, IEEE 802.11ah introduces several NDP frames, also known as short frames, such as short ACK, short block ACK, short CTS, and short PS-Poll, etc. The aim of these is to decrease the associated power consumption and medium occupancy.

3.2.3 Enhanced channel access mechanisms

In today's WLAN systems, where medium access is typically contention-based, the effectiveness of the channel access mechanism is significantly affected by the user contention levels. In IEEE 802.11 technology, the core channel access mechanism employs the Enhanced Distributed Channel Access (EDCA) scheme, which works efficiently with relatively small numbers of STAs and provides stochastic quality-of-service (QoS) differentiation. However, emerging MTC applications create challenges for next-generation IEEE 802.11 networks due to the large numbers of devices that need to be supported and, consequently, high levels of resulting contention. In IEEE 802.11ah, the EDCA has been modified to offer differentiated QoS to sensor STAs and non-sensor STAs. As a result, EDCA is the default access mechanism for the sub 1 GHz STA in 802.11ah.

In order to prevent from massive collisions, IEEE 802.11ah introduces a novel important channel access mechanism referred to as the *Restricted Access Window* (RAW) on top of the conventional EDCA scheme with Transmission Opportunity (EDCA TXOP). With the new RAW mechanism, the AP allocates a dedicated medium access period in the beacon interval, which is then divided into one or more time slots. The assignment of slots for specific STAs within the defined RAW is based on the TIM element in the beacon frames. The AP may also particular slots to the individual STA, or to a subset of STAs, for uplink and downlink traffic.

Due to the fact that additional overheads may arise from communication, IEEE 802.11ah technology introduces a new frame exchange protocol referred to as *Bi-Directional TXOP* (BDT) scheme, which reduces the protocol overhead. Compared to conventional access, BDT utilizes the current data frame as an ACK to the preceding data frame. Therefore, the BDT enables an AP and a non-AP STA to exchange a sequence of uplink and downlink frames within a reserved time.

3.2.4 Efficient interference mitigation schemes

One of the key introduced mechanisms to resolve the hidden terminal problem is *Sectorization*. Sectorization naturally partitions the coverage area of a Basic Service Set (BSS) into sectors, each containing a subset of STAs. This partitioning is achieved through a set of antennas, or a set of synthesized antenna beams, to cover various sectors of the BSS. The main goal of this mechanism is in reducing the interference between BSSs. Two types of sectorization schemes have been introduced by IEEE 802.11ah specifications: group sectorization and TXOP-based sectorization.

Another developed mechanism is *Sub-channel Selective Transmission* (SST) and Dynamic BW operation, where the goal is to mitigate interference due the excessive use of the channel, or resulting from an Overlapping BSS (OBSS) deployment. The primary channel is typically used by the network of a given BSS. It is static and may not change throughout the operation of the BSS. This common primary channel (usually 1 or 2 MHz) is employed by the STAs to communicate with the AP. However, due to varying channel conditions and STA locations, the levels of interference experienced on the primary channel may be considerably higher as compared to other available channels. Hence, SST will then enable a STA to select the best temporary channel among multiple SST-enabled operating channels to communicate with its peer STA.

4 Protocol Operation and Proposed Model

This section builds on the previous one to introduce the considered protocol operation features and explain the related simplifications.

4.1 IEEE 802.11ah Channel Access Protocol

When it comes to actual medium access, we expect that the BASIC channel access scheme (see Figure 2) would be preferred for most MTC scenarios to further reduce overheads. Additionally, sub 1 GHz STAs employ EDCA access, but in our paper we address a use-case where there is only one type of STAs and thus one type of traffic flow. Hence, QoS is not the main focus of our attention and a simpler Distributed Coordination Function (DCF) mechanism is addressed below instead of EDCA for the sake of simplicity.

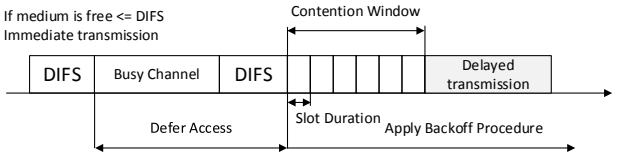

Figure 2 Example of BASIC access mechanism operation

According to the standard, for each device in the system, if there appears a new data packet (or an aggregated block of packets) in the buffer and there are no other transmissions sensed during the *DCF Interframe Space* (DIFS), the data transmission would be performed immediately after. Otherwise, medium access would be deferred according to the *Binary Exponential Backoff* (BEB) algorithm [49], which is used to resolve collisions, when there are more than one user transmitting data simultaneously.

On the other hand, if there is only one transmitting user, and in absence of other channel degradation factors, such a condition is called a *success*. Finally, if no device is transmitting, the channel is sensed *idle* (or empty). According to the protocol, for the *BASIC* mechanism in case of *collision* or corruption by the channel, the BEB operation is first applied. A uniformly-distributed *Backoff Counter (BC)* value is randomly chosen between zero and the Initial Contention Window W_0.

As the channel is sensed idle, the BC is decremented and eventually, when it reaches zero, the retransmission procedure commences. If a collision occurs again, the current *Contention Window* (CW) is doubled and the retransmission procedure is reinitialised as many times, as it is permitted by the *Retransmission Counter* (RC).

As there is a need to explicitly account for the unsaturated traffic behaviour by a large number of MTC devices in the considered system, we develop a corresponding analytical model and introduce it in what follows.

4.2 System Model and Main Assumptions

Here, we outline our proposed system model and its main assumptions. For the sake of exposition, we focus on the analysis of one MTC cluster and there are no hidden terminals assumed, as well as the channel is considered to be error-free. Important practical extensions to this baseline model are discussed in the subsequent sections.

For simplicity, we assume that the contention behaviour is similar for all of the MTC devices (i.e., they employ identical contention parameters). We further require that the start times of every slot are perceived synchronously by the users. We also assume that the overall system time is divided into very small equal-sized slots with the duration of t_g. These slots may be thought of as the atomic time intervals when a new packet generation is possible by the user.

Next, we define the *Event Duration*, where an event can be one of $s/c/e$ and is determined as follows.

(i) *Success*: If there is only one transmitting user in the system. The duration of such an event is defined as t_s, which is calculated according to the specifications as a sum of: DCF Interframe Space ($DIFS$); Data transmission duration; Short Interframe Space ($SIFS$), and Acknowledgment (ACK) duration.

(ii) *Idle*: If there is no transmission, the respective duration is taken as t_e, the slot duration.

(iii) *Collision*: If there is more than one simultaneously transmitting device, we consider a time interval t_c between the beginning of the transmission and the beginning of the next opportunity to transmit. It comprises: $DIFS$, $SIFS$, PHY timeout duration, Data transmission duration, and one idle slot duration.

Importantly, our model employs the exact number of opportunities for a user to generate a packet during every particular event duration ($L_{s/c/e}$). In other words, we sample the system operation time into smaller packet generation opportunities t_g, which also divide every event duration above. For example, for a success slot we can write $L_s = t_s/t_g$. For convenience, t_g is chosen such that $L_{s/c/e}$ are all integers.

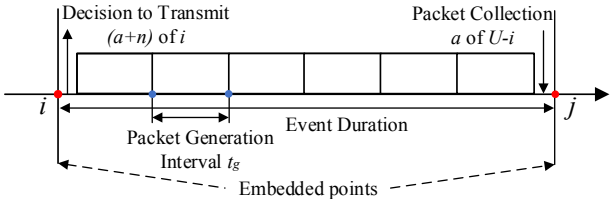

Figure 3 Event-based in-buffer packet arrival model

We concentrate on a particular number of users U associated with a single AP throughout the entire system operation time. With respect to the offered load, we assume Bernoulli arrivals [50] based on the packet generation intervals t_g as an approximation for the IoT-grade sensor network scenario discussed in [51]. Basically, this arrival flow type was chosen as a simple discrete-time stochastic process, when a device can generate a packet during the interval t_g with the probability σ. Upon a packet generation, the user would attempt its immediate transmission, if the packet has arrived into an empty buffer. Alternatively, at the packet generation event, there might already be a number of *backlogged users* i with packets ready for transmission. Backlogged users attempt their (re)transmissions with the probability p, which is the consequence of a prior unsuccessful transmission.

Let us observe an example operation of such a system for one particular event duration and the specified numbers of backlogged users i and j before and after, respectively (shown in Figure 3). Naturally, $n = \overline{0,i}$ users can attempt to send their packets based on the channel access probability p. The users without data in the buffer (a out of $U-i$) can generate new packets during every event duration. Importantly, a transition from i to j backlogged users is characterised differently for success and collision/empty events.

During a successful slot, $a = j-i-n-1$, $0 \le a \le U-i-n$. For the collision or empty events, $a = j-i-n$, $0 \le a \le U-i-n$. We assume that if the transmission is successful for a user, a new packet is not generated immediately. Hence, the generation procedure is applied starting with the following slot. Additionally, if a packet

is already generated during the current event duration, we assume that there would not be any new arrivals until the data packet is successfully transmitted by this user – our system operates in the lossless mode. This effectively allows for our users to be represented as buffers with the size of one to keep a single data packet.

5 Proposed Mathematical Analysis

In this section, we detail our analytical approach based on the consideration of the Markov chain at the appropriate *embedded points*. In what follows, we derive the state transition probability matrix and the corresponding stationary distribution vector. Basing on the latter, the key stationary system parameters may, in turn, be obtained, such as e.g., the number of backlogged users in the system. As our main performance indicators, we choose data throughput (taking into account only the data packets here, while excluding overheads) and channel access delay. Importantly, while delay itself may be of less interest for delay-tolerant MTC devices, it may be easily converted into energy efficiency, which is one of the useful system parameters for any MTC scenario.

5.1 Detailed System Analysis

From the data transmission standpoint, our system of interest operates in two alternative modes: when a new packet has just arrived – immediate transmission; or when a packet is being retransmitted using probabilistic channel access. The immediate transmission and the corresponding system events suggest the analysis by means of a two-dimensional Markov chain, which is able to take into account the past number of backlogged users (the system state) as it is shown in Figure 4.

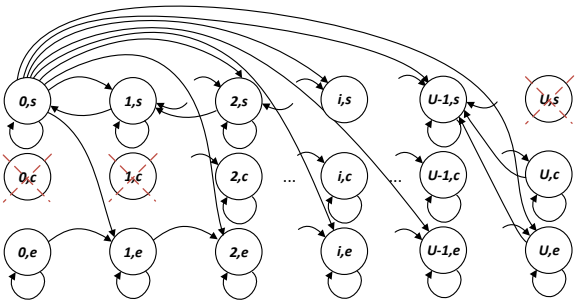

Figure 4 Underlying embedded Markov chain

More precisely, we consider a process $z(t)$ embedded at the beginning of every event (with a specified duration). Here, the state of the process is given as (i, x), where i is the number of backlogged users and x is the type of the previous event. Importantly, we remind that in our system three alternative events may occur: a collision, a successful transmission, and an empty slot.

To calculate the steady-state distribution of $z(t)$, we need to establish the transition probability matrix P

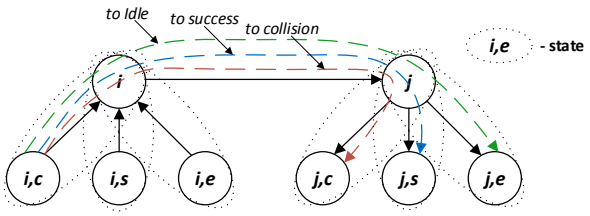

Figure 5 Simplified Markov chain for immediate transmission case

(represented in Table 1). Here, $P_{(i,x)\to(j,y)}$ is an element corresponding to the probability of a specific transition, as it is demonstrated in Figure 5, where all of the available state transitions for $i \to j$ are shown in more detail. To ease the understanding of our diagram, a detailed matrix is presented, where each of its cells is composed of specific conditions between two particular states.

Table 1 System states for immediate transmission

States (i/j)	**1**	**2**	**j**	**U+1**
1	$a_{1,1}$	$a_{1,2}$	$a_{1,j}$	$a_{1,U+1}$
2	$a_{2,1}$	$a_{2,3}$	$a_{2,j}$	$a_{2,U+1}$
..				
i	$a_{i,1}$	$a_{i,2}$	$a_{i,j}$	$a_{i,U+1}$
..				
U+1	$a_{U+1,1}$	$a_{U+1,2}$	$a_{U+1,j}$	$a_{U+1,U+1}$

State $a_{i,j}$	**j,s**	**j,c**	**j,e**
i,s	s_{11}	s_{12}	s_{13}
i,c	s_{21}	s_{23}	s_{23}
i,e	s_{31}	s_{33}	s_{33}

In what follows, we study individual system transitions.

Transition $(i, s) \to (j, s)$: For example, for a transition from the previous successful slot to the current successful slot to hold, there should be exactly one packet transmission

$$P_{(i,s)\to(j,s)} = \begin{cases} (1-p)^{j-1} pB(0, L_s|U-i), & j <= i, \\ (1-p)^{j} B(1, L_s|U-i), & i > j, \end{cases} \quad (1)$$

where L_s is the number of opportunities to generate a new packet for a user during the successful event. Here, $B_{s/c/e}(a, x|n)$ is such that there would be exactly a new arrivals during x number of slots, and n is the possible number of users to generate a packet, which can be calculated as

$$B_{s/c/e}(a, L_{s/c/e}|n) = \binom{n}{a} \rho_{s/c/e}^{a} (1-\rho_{s/c/e})^{n-a}, \quad (2)$$

where $\rho_{s/c/e}$ is the probability for a packet to be generated during an exactly chosen event duration, i.e., $\rho_{s/c/e} = 1 - (1-\sigma)^{L_{s/c/e}}$. For such a transition, it is clear that $j = i - 1$ if the packet has not been generated during the current transmission for this user, or $j = i$ otherwise.

Transition $(i, s) \to (j, e)$ from a successful state to an empty state can be obtained as

$$P_{(i,s)\to(j,e)} = B(0, L_s|U-i)(1-p)^i, \quad (3)$$

when none of the users decide to transmit in the current slot.

Transition $(i, s) \to (j, c)$: the last remaining transition may be calculated simply as

$$P_{(i,s)\to(j,c)} = \begin{cases} B_0(1-(1-p)^i - ip(1-p)^{i-1}), & k = 0, \\ B_1(1-(1-p)^i), & k = 1, \\ B(k, L_s|U-i), & k > 1, \end{cases} \quad (4)$$

where $k = j - i$, $B_1 = B(1, L_s|U-i)$, $B_0 = B(0, L_s|U-i)$.

All the following values in $P_{(i,x)\to(j,x)}$ sub-matrix may be calculated similarly, but the duration of the previous slot ($L_{s/c/e}$) should vary accordingly. Further, we calculate the stationary system distribution at the embedded points by means of solving the following system of linear equations

$$\boldsymbol{\pi}^{(0)} = P^T \boldsymbol{\pi}^{(0)}, \quad \boldsymbol{\pi}^{(0)} \boldsymbol{e} = 1, \quad (5)$$

where P is the transition probability matrix, $\boldsymbol{e} = (1, 1, ..., 1)$ is the vector of ones, and $\boldsymbol{\pi}^{(0)} = \left\{ \boldsymbol{\pi}^{(0)}_{(i,x)} : x = s/c/e, i = \overline{0, U} \right\}$.

Next, we derive the average duration of the next system event for the state (i, x) as

$$\overline{V}_{i,x} = \sum_{j=0}^{U} \sum_{y=c,s,e} P_{(i,x)\to(j,y)} L_y. \quad (6)$$

This, in turn, leads us to calculating the *aggregated stationary distribution in the form*

$$\boldsymbol{\Pi}_i = \frac{\boldsymbol{\pi}^{(0)}_{(i,s)} \overline{V}_{(i,s)} + \boldsymbol{\pi}^{(0)}_{(i,c)} \overline{V}_{(i,c)} + \boldsymbol{\pi}^{(0)}_{(i,e)} \overline{V}_{(i,e)}}{\sum_{j=0}^{U} \sum_{x=s,c,e} \boldsymbol{\pi}^{(0)}_{(j,x)} \overline{V}_{(j,x)}}, \quad (7)$$

where $\overline{V}_{i,x}$ is obtained from (6).

5.2 Main Performance Metrics

Given the underlying derivations above, we can now establish

$$E[N] = \sum_{i=0}^{U} i \boldsymbol{\Pi}_i. \quad (8)$$

In addition, we can obtain the average number of users

$$E[\acute{N}] = \sum_{x=s,c,e} \sum_{i=0}^{U} i \boldsymbol{\pi}^{(0)}_{i,x}. \quad (9)$$

Further, we may derive $S(i, x)$, which is the number of packets sent during the i^{th} event

$$S(i,x) = ip(1-p)^{i-1} B(0, L_x|U-i) + (1-p)^i B(1, L_x|U-i). \quad (10)$$

Finally, in order to calculate the system throughput, we have to find the number of data packets that can be sent per a packet generation interval

$$E[S] = \sum_{i=0}^{U} \sum_{x=s,c,e} S(i,x) \boldsymbol{\pi}^0_{(i,x)} \frac{1}{\overline{V}_{i,x}}. \quad (11)$$

Additionally, we have to characterize the number of data packets at the embedded points or per event

$$E[\acute{S}] = \sum_{i=0}^{U} \sum_{x=s,c,e} S(i,x) \boldsymbol{\pi}^0_{(i,x)}. \quad (12)$$

Hence, at this time we can calculate the number of bits sent per a packet generation interval, which translates into the system data throughput

$$R = \frac{E[S] l}{t_g}, \quad (13)$$

where l is the actual packet length in bytes and t_g is the packet generation duration in μs.

Importantly, we estimate the *packet delay* (μs) as a time interval between the generation event and the moment when the packet is transmitted successfully. Let f be the number of transmission attempts. Hence, the delay can be obtained as a sum of one success, $f - 1$ collisions, and $f - 1$ sets of idle slots after each collided transmission.

Ultimately, the delay expressed in the number of events may be derived using the Little's law as

$$E[\acute{T}] = 1 + \frac{E[\acute{N}]}{E[\acute{S}]} = = (f-1)\left(\frac{1}{p} - 1\right) + (f-1) + 1, \quad (14)$$

where $(1/p - 1)$ is the geometric average of idle slots after each collision. Hence, $f - 1 = p\frac{E[\acute{N}]}{E[\acute{S}]}$. This, in turn, leads to the actual data delay calculation (in μs)

$$E[T] = t_s + p\frac{E[\acute{N}]}{E[\acute{S}]}(t_c + \left(\frac{1}{p} - 1\right) t_e), \quad (15)$$

where $E[\acute{S}]$ is obtained via (12) and $E[\acute{N}]$ is given by (9).

Finally, for the effective power consumption estimation, we utilize the following equation

$$E = \int P^{(t)} dt = \\ = P_s t_s + (f-1) P_c t_c + (f-1) \left(\frac{1}{p} - 1 \right) t_e P_b, \quad (16)$$

where P_s, P_c, and P_e are the average power consumption levels for successful, collision, and empty slots in mW, respectively. The results are given in Figure 6 showing the energy consumption levels by varying the height of bars corresponding to the radio operation states.

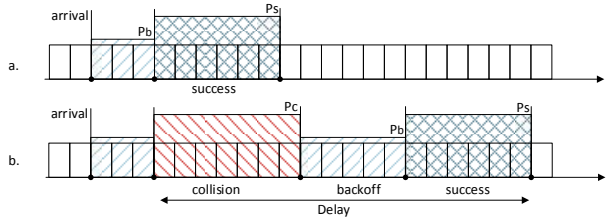

Figure 6 Power consumption estimation methodology

6 Considered Simulation Methodology

The initial parameters related to our simulations are taken from the system requirements document in [51]. In particular, the MAC- and PHY-layer settings are summarised in Table 2 and borrowed from [46], whereas most of the PHY-related features have been abstracted away by their inclusion into the corresponding timing values to reduce the performance evaluation complexity.

Table 2 Main system parameters

Parameter	Value
Packet size l	256 bytes
PHY data rate	0.65 Mbps
Number of users U	5 to 6000
Initial backoff window size (W_0)	16
Maximum contention window (CW_{max})	1024
Short retry limit (RC)	4
Simulation run duration	200 sec
DCF Interframe Space (DIFS)	264 μs
Short Interframe Space (SIFS)	160 μs
Physical layer timeout (PHY)	240 μs
Acknowledgment duration (ACK)	240 μs
Successful slot duration t_s	4264 μs
Collision slot duration t_c	4316 μs
Idle slot duration t_e	52 μs
Minimal packet generation period t_g	52 μs

6.1 Simulator Description and Verification

The system-level simulation environment employed here is an open source tool named OMNeT++ [52]. This general purpose simulation framework is based on C++ programming language with high programmability and rich protocol modelling capabilities. In particular, we utilised it for extending the existing IEEE 802.11 baseline implementation to support the necessary IEEE 802.11ah features. Evaluations were performed by employing our two computation clusters – both have 96GB of RAM, 10GB of Swap, two Intel(R) Xeon(R) CPU E5-2630 @ 2.30GHz with six cores each.

As a result, various MAC-layer access methods, including EDCA, DCF, PCF, and RAW, with their corresponding parameters can be easily simulated and assessed. Different channel and path loss models for indoor and outdoor scenarios, as described by IEEE 802.11ah specification, can be additionally tested. Further, a variety of Modulation and Coding Schemes (MCSs) can be flexibly evaluated. Generally, the OMNeT++ platform has been used in the past for implementation of numerous wireless protocols [53].

An extensive validation of the discussed tool in the context of IEEE 802.11ah technology has already been done in [54]. There, the verification focused on the evaluation of the system throughput and power consumption for basic (i.e., DCF) access mechanism with and without RAW, where saturated traffic has been assumed. The simulated results were compared to the well-established analytical expressions for saturated throughput from [49] and a perfect match between both types of results was observed by the authors.

6.2 Current Numerical Results

As follows from the previous (sub-)sections, our approach constitutes a powerful framework, which is equally applicable for saturated and unsaturated systems with a large number of users for BASIC asses mode. In what follows, we first evaluate the total number of successfully sent data units (transmissions) per slot, which is then converted into the actual system throughput (as per (13)).

Note in Figure 7 that presently the simulation-based values see difficulty in producing results for very large numbers of users (due to exceptionally high simulation complexity), while at the same time demonstrate excellent convergence with our analysis for lower node densities. Hence, our analytical methodology is employed here to make a performance prediction for up to 6000 MTC devices. Here, the packet generation probability is static – a data packet can be generated once in about every 10 s. Naturally, the exact generation period can be calculated as $1/\sigma \cdot t_g$ and the corresponding output results are produced by (13).

Further, by taking into account the proposed RAW mechanism as part of our evaluation methodology, we may shed light on some of the most advanced and

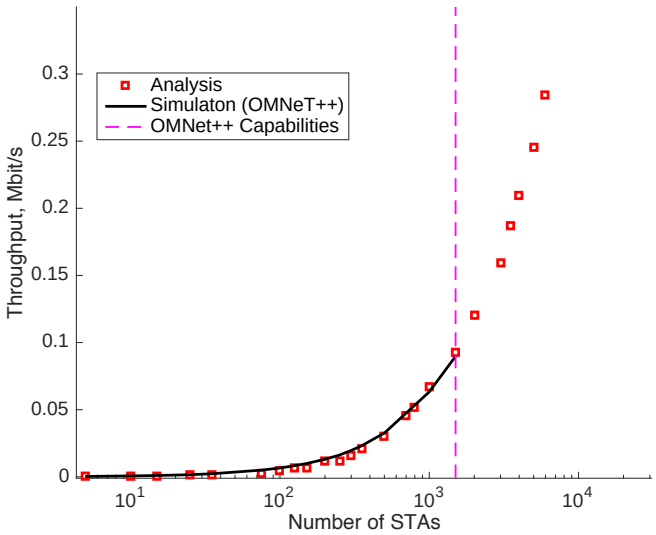

Figure 7 Throughput for different numbers of users operating in unsaturated mode (the average packet generation period is 10 s)

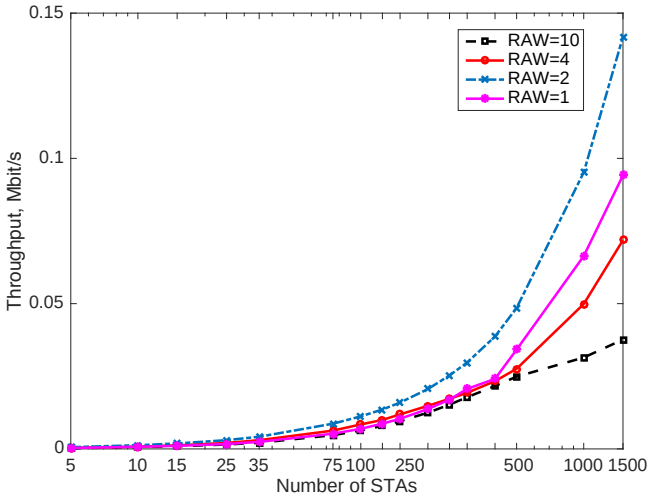

Figure 8 Throughput for different numbers of RAW periods

novel specific features of the 802.11ah technology. We compare our model with the simulation results obtained for different numbers of RAWs, see Figure 8. Clearly, the proposed analytical model and the employed low packet arrival rate demonstrate similar system throughput behaviour for small numbers of RAW periods. However, this would change as the number of windows increases. This effect is due to the fact that a device is likely to be in sleep mode when the packet is generated and sent to its buffer. Importantly, for high numbers of RAWs and users, the first transmission is more seldom and thus the system converges to saturation more rapidly. Therefore, the proposed analytical model may have some limitations due to possible system unfairness, as it is designed for reasonably low arrival rates.

Given that the exact RAW protocol operation remains largely vendor-specific, we employ an implementation-independent evaluation metric in the form of the conditional collision probability (conditioning on the fact that the STA has transmitted). Our RAW-centric scenario follows the guidelines in [51] with (7) and results in Figure 9, which confirms the intuition on that RAW grouping may decrease collision probability in the system. Here, we assume that the device is not generating new data (sleeping) during the RAW transmission intervals other than its own. Therefore, we increase the arrival flow rate and analyse alternative RAW settings, for a given total number of MTC devices. The figure shows how a particular configuration affects the collision probability and helps select appropriate RAW parameters as it clearly characterises the trends of growth in data collisions and thus saturation. This plot also highlights the benefits of our analytical framework, as it can model systems with very different inter-arrival times and deliver fine-grained probabilities.

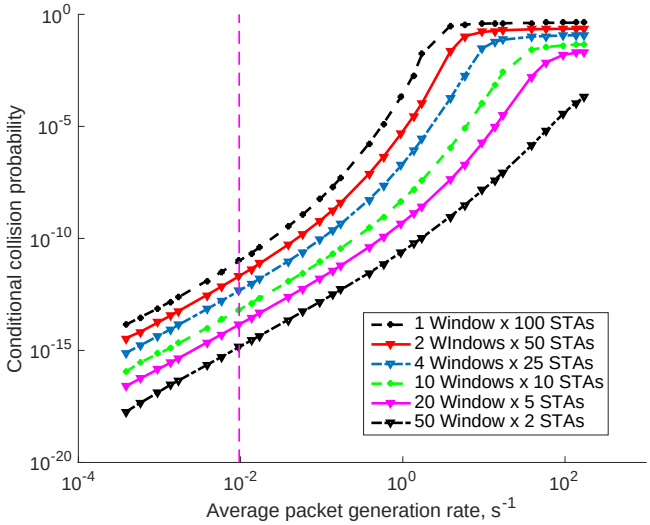

Figure 9 Conditional collision probability vs. MTC data arrival rate

Furthermore, we estimate the effective power consumption per a successfully transmitted packet with (16) for the case when the RAW is not used. It is calculated as the overall power consumption from the end of the packet generation event and until the data is transmitted successfully. The power-related values are taken from [54]: 255 mW for transmission, 135 mW for reception and channel sensing, and 1.5 mW for the sleep mode. The output results are summarised by Table 3. Importantly, the actual collision rate directly impacts the relative difference between our simulations and analysis. With more MTC devices in the system, simulation results demonstrate higher instability, whereas our analysis assumes averaged steady-state system operation.

To further support this discussion, in Figure 10 we increase the arrival traffic arrival rate and analyse the near-saturation conditions for selected MTC scenarios. While the analytical model proposed in this work is not intended to address the full-buffer case, we can clearly see

Table 3 Effective Power Consumption (results for simulation and analysis are given in mW per packet)

Number of nodes	Simulation	Analysis	Relative Difference
100	1.01	1.008	0.24%
500	1.023	1.017	0.56%
1000	1.055	1.039	1.59%
1500	1.203	1.104	8.92%

that for the packet generation periods of greater than 10 seconds, saturation does not happen for typical settings. For example, let us focus on the blue curve ($t_g = 1s$) as we observe two extrema in the plot. The first one is around 150 nodes, and it clearly demonstrates when the BEB (Binary Exponential Backoff) procedure takes effect, i.e. when the devices are beginning to collide and thus increase the retransmission time. The second one is around 400 nodes and represents the worst case, when all of the devices are in deep retransmission phases most of the time and continue to collide. The region after 500 nodes reflects the utilization of suboptimal BEB parameters for the exact number of STAs, that is, when the collision resolution rate is faster than the emergence of new collisions.

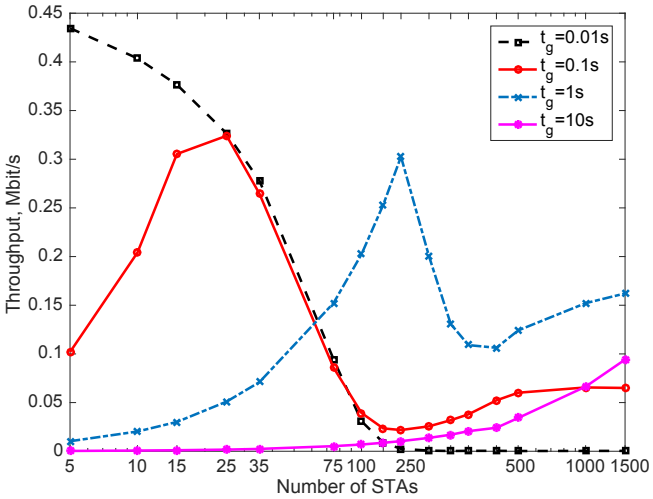

Figure 10 Throughput in near-saturation cases

Finally, in Figure 11 we evaluate the feasibility of OMNet++ simulator runtime for our employed computation cluster. Even for just 1500 MTC devices, it may already require up to 14 hours of computational time for just one round of simulations, and it is only expected to exponentially grow further as more users are added into the system. This excessive time consumption undeniably advocates for the benefits of our proposed analysis in contrast to highly-demanding simulations.

7 Conclusion

In this work, we summarised the potential offered by the emerging IEEE 802.11ah specifications to support the massive MTC deployments. Correspondingly, we

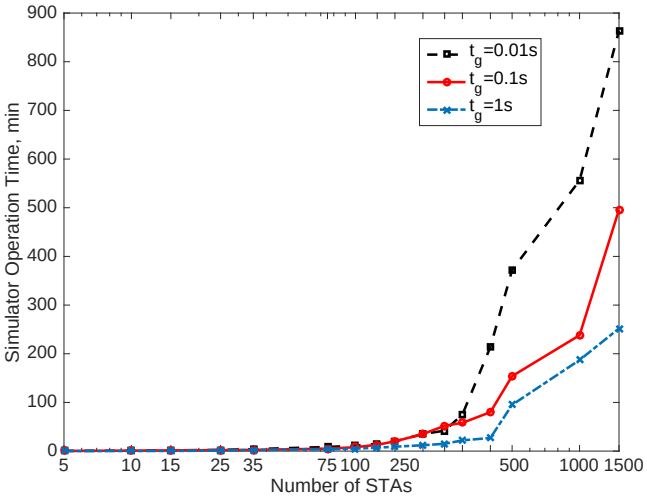

Figure 11 Typical simulation times in our experiments

proposed a novel analytical model that characterises system throughput, delay, and power consumption for a large number of MTC devices communicating over IEEE 802.11ah technology in unsaturated mode. Our mathematical framework has been verified by an advanced simulation tool, OMNeT++, and has been shown to offer adequate performance predictions even in the scenarios where simulation has limited capability due to increasing numerical complexity.

Further, we analysed the key RAW (Restricted Access Window) scheme of IEEE 802.11ah that allows to reduce the impact of collisions and thus improve system performance. In particular, we considered possible groupings of 100 devices and respective collision probability values. Effective power consumption per a transmitted packet has also been obtained. Importantly, relative difference observed between our simulation (OmNet++) and analysis (Markov chains) is within 10% of the effective power consumption. As our future work, we plan to extend our model with a spatial component, which would allow to capture more realistic multi-cluster deployment scenarios, as well as implement more advanced features of IEEE 802.11ah protocol.

References

[1] Steve Whitehead. Adopting wireless machine-to-machine technology. *IEEE Computing and Control Engineering Journal*, 15(5):40–46, 2004.

[2] Behnam Badihi, Luis Felipe Del Carpio, Parth Amin, Anna Larmo, Miguel Lopez, and Dee Denteneer. Performance Evaluation of IEEE 802.11ah Actuators. In *Proc. of IEEE 83rd Vehicular Technology Conference (VTC Spring), 2016*, pages 1–5. IEEE, 2016.

[3] Yan Zhang, Rong Yu, Maziar Nekovee, Yi Liu, Shengli Xie, and Stein Gjessing. Cognitive Machine-to-Machine Communications: Visions and Potentials for the Smart Grid. *IEEE Network*, 26(3):6–13, 2012.

[4] Massimo Condoluci, Leonardo Militano, Antonino Orsino, Jesus Alonso-Zarate, and Giuseppe Araniti. LTE-direct vs. WiFi-direct for machine-type communications over LTE-A systems. In *Proc. of 26th Annual International Symposium on Personal, Indoor, and Mobile Radio Communications (PIMRC)*, pages 2298–2302. IEEE, 2015.

[5] Toni Adame, Alain Bel, Boris Bellalta, Jaume Barcelo, and Miquel Oliver. IEEE 802.11ah: the WiFi approach for M2M communications. *IEEE Wireless Communications*, 21(6):144–152, 2014.

[6] Evgeny Khorov, Andrey Lyakhov, Alexander Krotov, and Andrey Guschin. A survey on IEEE 802.11ah: An enabling networking technology for smart cities. *Computer Communications*, 58:53–69, 2015.

[7] Peter Rysavy. Meeting mobile demand with a combination of spectrum alternatives. *IEEE Wireless Communications*, 21(2):6–7, 2014.

[8] Minyoung Park. IEEE 802.11ah: sub-1-GHz license-exempt operation for the internet of things. *IEEE Communications Magazine*, 53(9):145–151, 2015.

[9] Chin Sean Sum, Hiroshi Harada, Fumihide Kojima, Zhou Lan, and Ryuhei Funada. Smart Utility Networks in TV White Space. *IEEE Communications Magazine*, 49(7):132–139, 2011.

[10] Stefan Aust. A Framework for Massive Access and Radio Resource Management in Urban WLANs. In *Proc. of IEEE 38th Conference on Local Computer Networks Workshops (LCN Workshops)*, pages 93–99, 2013.

[11] Stefan Aust and Tetsuya Ito. Sub 1GHz Wireless LAN Deployment Scenarios and Design Implications in Rural Areas. In *Proc. of IEEE Globecom 2011 Workshop on Rural Communications-Technologies, Applications, Strategies and Policies*, pages 1045–1049, 2011.

[12] Stefan Aust, Venkatesha Prasad, and Ignas GMM Niemegeers. IEEE 802.11ah: Advantages in standards and further challenges for sub 1 GHz Wi-Fi. In *Proc. of 2012 IEEE International Conference on Communications (ICC)*, pages 6885–6889. IEEE, 2012.

[13] Stefan Aust and Venkatesha Prasad. IEEE 802.11ah: Advantages in Standards and Further Challenges for Sub 1 GHz Wi-Fi. In *Proc. of IEEE International Conference onCommunications (ICC)*, pages 6885–6889, 2012.

[14] Stefan Aust and Venkatesha Prasad. Analysis of the Performance Boundaries of Sub-1 GHz WLANs in the 920 MHz ISM-Band. In *Proc. of Tenth International Symposium on Wireless Communication Systems (ISWCS 2013)*, pages 1–5, 2013.

[15] Ali Hazmi, Jukka Rinne, and Mikko Valkama. Feasibility Study of IEEE 802.11ah Radio Technology for IoT and M2M use Cases. In *Proc. of Second International Workshop on Machine-to-Machine Communications*, pages 1687–1692, 2012.

[16] Behnam Badihi Olyaei, Juho Pirskanen, Orod Raeesi, Ali Hazmi, and Mikko Valkama. Performance Comparison Between Slotted IEEE 802.15.4 and IEEE 802.11ah in IoT Based Applications. In *Proc. of IEEE 9th International Conference on Wireless and Mobile Computing, Networking and Communications (WiMob)*, pages 332–337, 2013.

[17] Toni Adame, Albert Bel, Boris Bellalta, Jaume Barceló, Javier Gonzalez, and Miquel Oliver. Capacity Analysis of IEEE 802.11ah WLANs for M2M Communications. In *Multiple Access Communcations*, pages 139–155. Springer International Publishing, 2013.

[18] Weiping Sun, Munhwan Choi, and Sunghyun Choi. IEEE 802.11ah: A Long Range 802.11 WLAN at Sub 1 GHz. *Journal of ICT Standardization*, 1:1–26, 2013.

[19] Yuan Zhou, Haiguang Wang, Shoukang Zheng, and Zander Zhongding Lei. Advances in IEEE 802.11ah Standardization for Machine-Type Communications in Sub-1GHz WLAN. In *Proc. of IEEE Second Workshop on Telecommunication Standards*, pages 1269–1273, 2013.

[20] Evgeny Khorov, Alexander Krotov, and Andrey Lyakhov. Modelling machine type communication in IEEE 802.11ah networks. In *Proc. of International Conference on Communication Workshop (ICCW)*, pages 1149–1154. IEEE, 2015.

[21] Oghenekome Oteri, Pengfei Xia, Frank Lasita, and Robert Olesen. Advanced Power Control Techniques for Interference Mitigation in Dense 802.11 Networks. In *Proc. of 16th International Symposium on Wireless Personal Multimedia Communications (WPMC)*, pages 1–7, 2013.

[22] Hyun Ho Choi, Jung Min Moon, In Ho Lee, and Howon Lee. Carrier Sense Multiple Access with Collision Resolution. *IEEE Communications Letters*, 17(6):1284–1287, 2013.

[23] Albert Bel, Toni Adame, Boris Bellalta, Jaume Barcelo, Javier Gonzalez, and Miquel Oliver. CAS-based Channel Access Protocol for IEEE 802.11ah WLANs. In *Proc. of European Wireless Conference (EW)*, pages 1–6, 2014.

[24] Lei Zheng, Lin Cai, Jianping Pan, and Minming Ni. Performance Analysis of Grouping Strategy for Dense IEEE 802.11 Networks. In *Proc. of IEEE Global Communications Conference (GLOBECOM)*, pages 219–224, 2013.

[25] Lei Zheng, Minming Ni, Lin Cai, Jianping Pan, Chittabrata Ghosh, and Klaus Doppler. Performance analysis of group-synchronized DCF for dense IEEE 802.11 networks. *IEEE Transactions on Wireless Communications*, 13(11):6180–6192, 2014.

[26] Monisha Ghosh and Frank Lasita. Puncturing of CRC Codes for IEEE 802.11ah. In *Proc. of IEEE 78th Vehicular Technology Conference (VTC Fall)*, pages 2–6, 2013.

[27] Hsiang-ho Lin. DeepSleep: IEEE 802.11 Enhancement for Communications. In *Proc. of Global Communications Conference (GLOBECOM)*, pages 5231–5236, 2012.

[28] Ren Ping Liu, Gordon Sutton, and Iain Collings. Power Save with Offset Listen Interval for IEEE 802.11ah Smart Grid Communications. In *Proc. of IEEE International Conference on Communications (ICC)*, pages 4488–4492, 2013.

[29] Ioannis Glaropoulos, Stefan Mangold, and Vladimir Vukadinovic. Enhanced IEEE 802.11 Power Saving for Multi-hop Toy-to-Toy Communication. In *Proc. of IEEE International Conference on Cyber, Physical and Social Computing*, pages 603–610. IEEE, August 2013.

[30] Kohei Ogawa, Yuki Sangenya, Masahiro Morikura, Koji Yamamoto, and Tomoyuki Sugihara. IEEE 802.11ah Based M2M Networks Employing Virtual Grouping and Power Saving Methods. In *Proc. of IEEE 78th Vehicular Technology Conference (VTC Fall)*, pages 1–5, 2013.

[31] Ren Ping Liu, Gordon Sutton, and Iain Collings. WLAN Power Save with Offset Listen Interval for Machine-to-Machine Communications. *IEEE Transactions on Wireless Communications*, 13(5):2552–2562, 2014.

[32] Giuseppe Bianchi and Ilenia Tinnirello. Remarks on IEEE 802.11 DCF performance analysis. *IEEE Communications Letters*, 9(8):765–767, 2005.

[33] Juki Wirawan Tantra, Chuan Heng Foh, Ilenia Tinnirello, and Giuseppe Bianchi. Analysis of the IEEE 802.11e EDCA under statistical traffic. In *IEEE International Conference on Communications*, volume 2, pages 546–551. IEEE, 2006.

[34] Churong Chen and Choi Look Law. Throughput performance analysis and experimental evaluation of IEEE 802.11b radio link. In *Proc. of AFIPS, Fall Joint Comput. Conference of 6th International Conference on Information, Communications & Signal Processing*, pages 1–5. IEEE, 2007.

[35] Fred Daneshgaran, Massimiliano Laddomada, Fabio Mesiti, and Marina Mondin. Unsaturated throughput analysis of IEEE 802.11 in presence of non ideal transmission channel and capture effects. *IEEE Transactions on Wireless Communications*, 7(4):1276–1286, 2008.

[36] Ali Hazmi, Luis Felipe Del Carpio, Ahmet Goekceoglu, Behnam Badihi, Parth Amin, Anna Larmo, Mikko Valkama, et al. Duty Cycle Challenges of IEEE 802.11ah Networks in M2M and IoT Applications. In *Proc. of 22th European Wireless Conference European Wireless*, pages 1–7. VDE, 2016.

[37] Mengxi Dong, Zhanji Wu, Xiang Gao, and Huan Zhao. An efficient spatial group restricted access window scheme for IEEE 802.11 ah networks. In *Proc. of 2016 Sixth International Conference on Information Science and Technology (ICIST)*, pages 168–173. IEEE, 2016.

[38] Weiping Sun, Munhwan Choi, and Sunghyun Choi. IEEE 802.11ah: A long range 802.11 WLAN at sub 1 GHz. *Journal of ICT Standardization*, 1(1):83–108, 2013.

[39] Pasquale Scopelliti, Giuseppe Araniti, Gabriel-Miro Muntean, and Antonio Iera. Mobility-aware energy-quality trade-off for video delivery in dense heterogeneous networks. In *Proc. of IEEE International Symposium on Broadband Multimedia Systems and Broadcasting (BMSB)*, pages 1–6. IEEE, 2016.

[40] Byoung Hoon Jung, Nah-Oak Song, and Dan Keun Sung. A network-assisted user-centric WiFi-offloading model for maximizing per-user throughput in a heterogeneous network. *IEEE Transactions on Vehicular Technology*, 63(4):1940–1945, 2014.

[41] Gabor Fodor, Stefan Parkvall, Stefano Sorrentino, Pontus Wallentin, Qianxi Lu, and Nadia Brahmi. Device-to-device communications for national security and public safety. *IEEE Access*, 2:1510–1520, 2014.

[42] Giuseppe Bianchi. IEEE 802.11-saturation throughput analysis. *IEEE Communications Letters*, 2(12):318–320, 1998.

[43] Behnam Badihi Olyaei, Juho Pirskanen, Orod Raeesi, Ali Hazmi, and Mikko Valkama. Performance comparison between slotted IEEE 802.15.4 and IEEE 802.11ah in IoT based applications. In *Proc. of IEEE 9th International Conference on Wireless and Mobile Computing, Networking and Communications (WiMob)*, pages 332–337. IEEE, 2013.

[44] Gabor Fodor, Stefano Sorrentino, and Shabnam Sultana. Network assisted device-to-device communications: use cases, design approaches, and performance aspects. In *Smart Device to Smart Device Communication*, pages 135–163. Springer, 2014.

[45] Dung Pham Van, Bhaskar Prasad Rimal, Martin Maier, and Luca Valcarenghi. Design, Analysis, and Hardware Emulation of a Novel Energy Conservation Scheme for Sensor Enhanced FiWi Networks (ECO-SFiWi). *IEEE Journal on Selected Areas in Communications*, 34(5):1645–1662, 2016.

[46] IEEE. Proposed TGah Draft Amendment. `https://mentor.ieee.org/802.11/documents?is_group=00ah`, August 2016.

[47] Ali Hazmi, Jukka Rinne, and Mikko Valkama. Feasibility study of IEEE 802.11ah radio technology for IoT and M2M use cases. In *Proc. of IEEE Globecom Workshops*, pages 1687–1692. IEEE, 2012.

[48] Anna Follmann, Mario Nascimento, Andreas Züfle, Matthias Renz, Peer Kröger, and Hans-Peter Kriegel. Continuous probabilistic count queries in wireless sensor networks. In *Proc. of International Symposium on Spatial and Temporal Databases*, pages 279–296. Springer, 2011.

[49] Giuseppe Bianchi. Performance Analysis of the IEEE 802.11 Distributed Coordination Function. *IEEE Journal on Selected Areas in Communications*, 18, no. 3:535–547, 2000.

[50] Mikhail Gerasimenko, Vitaly Petrov, Olga Galinina, Sergey Andreev, and Yevgeni Koucheryavy. Impact of machine-type communications on energy and delay performance of random access channel in LTE-advanced. *Transactions on Emerging Telecommunications Technologies*, 24(4):366–377, 2013.

[51] IEEE. TGah Functional Requirements and Evaluation Methodology Rev. 4. https://mentor.ieee.org/802.11/dcn/11/11-11-0905-04-00ah-tgah-functional-requirements-and-evaluation-methodology.doc, 2011.

[52] OMNeT++. Online User Manual. `http://www.omnetpp.org/doc/omnetpp/manual/usman.html`, 2001-14.

[53] Muhammad Qutab-ud din, Ali Hazmi, Behnam Badihi, Anna Larmo, Johan Torsner, and Mikko Valkama. Performance analysis of IoT-enabling IEEE 802.11ah technology and its RAW mechanism with non-cross slot boundary holding schemes. In *Proc. of 16th International Symposium on a World of Wireless, Mobile and Multimedia Networks (WoWMoM)*, pages 1–6. IEEE, 2015.

[54] Orod Raeesi, Juho Pirskanen, Ali Hazmi, Toni Levanen, and Mikko Valkama. Performance evaluation of IEEE 802.11ah and its restricted access window mechanism. In *Proc. of Communications Workshops (ICC)*, pages 460–466, 2014.